

THE ‘SAUSAGE’ GLOBULAR CLUSTERS

G. C. MYEONG¹, N. W. EVANS¹, V. BELOKUROV¹, J. L. SANDERS¹ AND S. E. KOPOSOV^{1,2}

¹Institute of Astronomy, University of Cambridge, Madingley Road, Cambridge CB3 0HA, United Kingdom

²McWilliams Center for Cosmology, Department of Physics, Carnegie Mellon University, 5000 Forbes Avenue, Pittsburgh PA 15213, USA

Draft version July 3, 2018

ABSTRACT

The *Gaia Sausage* is an elongated structure in velocity space discovered by Belokurov et al. (2018) using the kinematics of metal-rich halo stars. It was created by a massive dwarf galaxy ($\sim 5 \times 10^{10} M_{\odot}$) on a strongly radial orbit that merged with the Milky Way at a redshift $z \lesssim 3$. We search for the associated *Sausage Globular Clusters* by analysing the structure of 91 Milky Way globular clusters (GCs) in action space using the *Gaia* Data Release 2 catalogue, complemented with *Hubble Space Telescope* proper motions. There is a characteristic energy E_{crit} which separates the *in situ* objects, such as the bulge/disc clusters, from the accreted objects, such as the young halo clusters. There are 15 old halo GCs that have $E > E_{\text{crit}}$. Eight of the high energy, old halo GCs are strongly clumped in azimuthal and vertical action, yet strung out like beads on a chain at extreme radial action. They are very radially anisotropic ($\beta \sim 0.95$) and move on orbits that are all highly eccentric ($e \gtrsim 0.80$). They also form a track in the age-metallicity plane distinct from the bulk of the Milky Way GCs and compatible with a dwarf spheroidal origin. These properties are consistent with GCs associated with the merger event that gave rise to the *Gaia Sausage*.

Keywords: galaxies: kinematics and dynamics — galaxies: structure

1. INTRODUCTION

There are multiple and striking pieces of evidence for the existence of a massive ancient merger which provides the bulk of the stars in the inner halo of the Milky Way galaxy. For example, the radial density profile of the stellar halo shows a dramatic break at around 30 kpc in tracers such as RR Lyrae and blue horizontal branch stars (e.g., Watkins et al. 2009; Deason et al. 2011). Deason et al. (2013) argued that this could be interpreted as the last apocentre of a massive progenitor galaxy accreted between 8 and 10 Gyr ago. Myeong et al. (2018a) showed that the kinematics of metal-rich halo stars ($-1.9 < [\text{Fe}/\text{H}] < -1.1$) betray extensive evidence of recent accretion using the SDSS-*Gaia* catalogue. The variation in Oosterhoff classes of RR Lyraes with radius (Belokurov et al. 2018a) similarly shows evidence that the bulk of the field RRab is provided by a single massive progenitor. Finally, Belokurov et al. (2018b) demonstrated that the shape of the velocity ellipsoid of the inner metal-rich stellar halo is highly non-Gaussian and sausage-shaped. They interpreted this *Gaia Sausage* as evidence that two thirds of the local stellar halo could have been deposited via the disruption of a massive ($\gtrsim 10^{10} M_{\odot}$) galaxy on a strongly radial orbit between redshift $z = 3$ and $z = 1$. Although identified in the SDSS-*Gaia* catalogue, recent investigations by Haywood et al. (2018) with the new *Gaia* Data Release 2 (DR2) catalogue (Gaia Collaboration et al. 2018) support the original hypothesis. If so, then this beast must have brought with it a population of globular clusters (GCs), now dispersed in the inner halo. After all, the similarly massive Sagittarius galaxy (Sgr) is now known to have brought at least 4 and possibly 7 GCs with it (e.g., Forbes & Bridges 2010; Sohn et al. 2018).

The main aim of this *Letter* is to search for the *Sausage Globular Clusters*. The identification of objects accreted

in the same merger event is easiest in action space. Actions have the property of adiabatic invariance, so that they stay approximately constant when changes in the potential occur slowly (e.g., Goldstein 1980; Binney & Spergel 1982). Globular clusters accreted in the same event are identifiable as clumped and compact substructures in action space (as is indeed the case for the 4 Sgr GCs – Terzan 7, Terzan 8, Arp 2, Pal 12). Historically, actions were cumbersome to calculate, but recent theoretical advances have transformed the situation (e.g., Binney 2012; Sanders & Binney 2016). The power of actions has recently been demonstrated by the identification of the tidal disorgements of ω Centauri (Myeong et al. 2018b). Here, we display the Milky Way globular clusters in action space using a realistic Galactic potential comprising flattened stellar and gas discs, halo and bulge (McMillan 2017) with the specific aim of identifying the *Sausage Globular Clusters*.

2. THE GLOBULAR CLUSTERS IN ACTION SPACE

The Milky Way globular clusters are a disparate group: some were formed *in situ* in the Milky Way, some acquired by the engulfment of dwarf galaxies. A classification was introduced by Zinn (1993), in which globular clusters are divided into bulge/disc, old halo and young halo on the basis of cluster metallicity and horizontal branch morphology. The bulge/disc systems are concentrated in the Galactic bulge and inner disc, whilst the old halo clusters are predominantly in the inner halo. They are mostly believed to have been formed in the Milky Way, though ~ 15 – 17 per cent might have been accreted. The young halo clusters can extend to large radii and are all believed to have been accreted (see e.g., Mackey & Gilmore 2004; Mackey & van den Bergh 2005).

The combination of observables from the Gaia Collaboration et al. (2018), Sohn et al. (2018) and Harris (1996, 2010 edition) allows us to obtain full six-dimensional in-

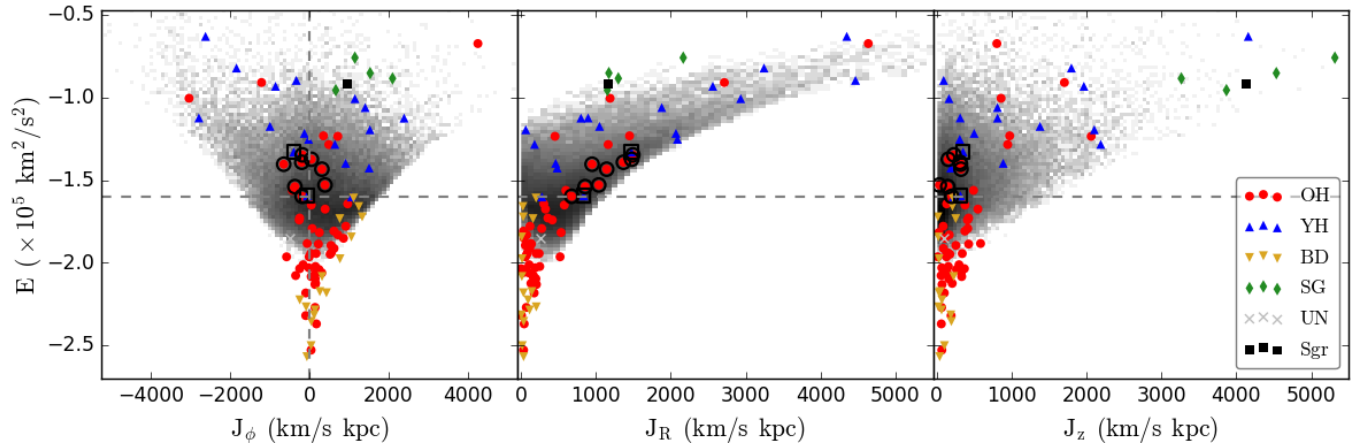


Figure 1. The distribution of globular clusters (GCs) in energy-action space or (J_ϕ, E) , (J_R, E) and (J_z, E) space. The grey-scale background shows the halo main-sequence turn-off (MSTO) stars from Myeong et al. (2018a) as a comparison. There are 75 GCs with *Gaia* DR2 proper motions and a further 16 with *Hubble Space Telescope* proper motions; 53 old halo (OHs, red circles), 17 young halo (YHs, blue triangles), 16 bulge/disc (BDs, yellow triangles), and 4 Sgr GCs (SG, green diamonds) together with 1 of unknown classification (grey cross). The Sagittarius galaxy (Sgr) is also marked as a black filled square. The vertical dashed line marks the division between prograde ($J_\phi > 0$) and retrograde ($J_\phi < 0$). The horizontal dashed line signifies the characteristic energy above which all the YHs lie, and below which all the BDs lie. The eight OH globular clusters whose symbols are enclosed by black open circles are grouped together in (J_ϕ, E) and (J_z, E) , whilst in (J_R, E) they are stretched out close to the boundary of J_R at corresponding energy (as judged from the MSTOs). They are the Sausage GCs. The 2 YHs enclosed with black open squares form an extended selection that may also be related. They have horizontal branch morphology similar to OHs, and have similar actions.

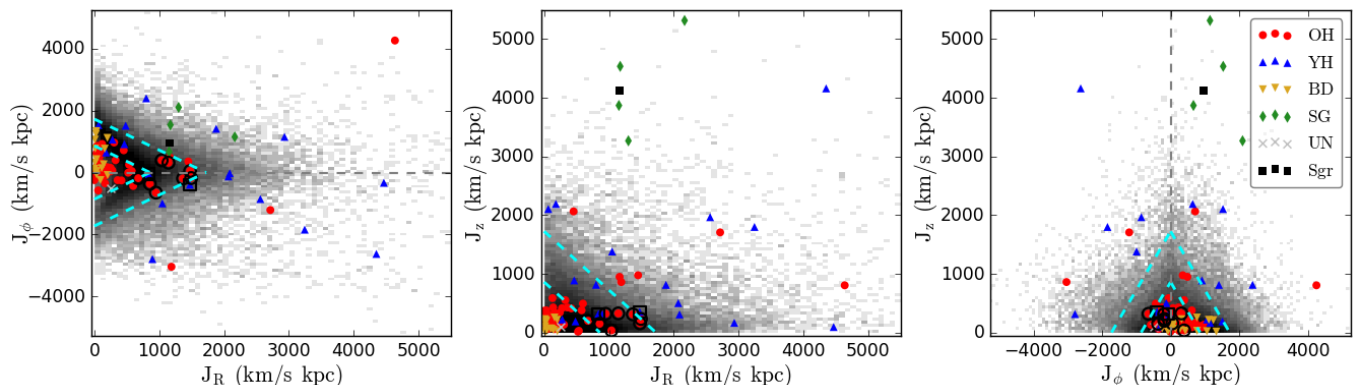


Figure 2. The same data as Fig. 1, but now in action space. The Sausage GCs form an extended sequence in J_R , but are tightly clustered in J_ϕ and especially J_z . Again black circles enclose probable members, black open squares possible; red circles are OHs, blue triangles are YHs, yellow triangles are BDs, green diamonds are SGs and grey cross is unknown. The black filled square is Sgr itself. The grey dashed line marks $J_\phi = 0$. The two cyan dashed lines mark two constant-energy surfaces projected onto the principal planes to provide a rough idea of the action space morphology (see e.g., Figure 3.25 of Binney & Tremaine 2008).

formation for 91 globular clusters (out of a total of ~ 150 in the Galaxy). To convert from observables to the Galactic rest-frame, we use the circular speed of 232.8 km s^{-1} at the Sun’s position of 8.2 kpc , consistent with the McMillan (2017) potential, whilst for the Solar peculiar motion we use the most recent value from Schönrich et al. (2010), namely $(U, V, W) = (11.1, 12.24, 7.25) \text{ km s}^{-1}$. These values differ from those used by the Gaia Collaboration et al. (2018) or Posti & Helmi (2018), so there are small differences in quantities such as apocentres and eccentricities. We use the numerical method of Binney (2012) and Sanders & Binney (2016) to compute the action variables of each globular cluster (J_R, J_ϕ, J_z). Globular clusters associated with the Gaia Sausage must lie on highly radial orbits, and so have low J_ϕ and J_z , but very large J_R . The uncertainty in proper motions is the main contributor to the median (total) velocity error of $\sim 9 \text{ km s}^{-1}$. This leads to median errors in the actions

of $\sim 10\%$, and so features in action space are robust against uncertainties. Fig. 1 presents the distribution of globular clusters in energy and action space, while Fig. 2 presents the projections onto the principal planes of action space. In both cases, we also show as grey pixels the distribution of main sequence turn-off stars (MSTOs) from Myeong et al. (2018a). This is to give an idea of the range in action at any energy level occupied by the stellar halo. Both plots are colour-coded according to the conventional classification from Mackey & van den Bergh (2005): red circles mark the old halo globular clusters (OHs), the blue triangles the young halo globular clusters (YHs), yellow triangles the bulge/disc ones (BDs) and green diamonds the Sagittarius GCs (SG). The Sagittarius dwarf (Sgr) is also marked as a black filled square. The young halo globular clusters all lie above a critical energy of $E_{\text{crit}} = -1.6 \times 10^5 \text{ km}^2 \text{ s}^{-2}$. The bulge/disc globulars all lie below this critical energy. We regard the

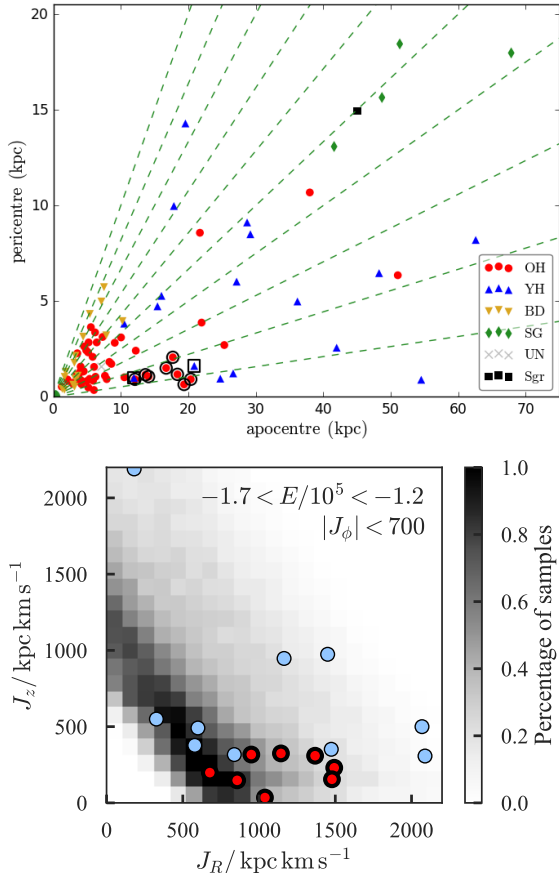


Figure 3. Upper Panel: Apocentres and pericentres of the GCs, colour coded according to old halo (red circles), young halo (blue triangles), bulge/disc (yellow triangles), Sgr GCs (green diamonds), and unknown (grey cross). Sagittarius galaxy (Sgr) is also marked (black filled square). Lines of constant eccentricity from 0 to 0.9 in steps of 0.1 are shown in green. Note the Sausage GCs (black open circles as probables and open squares as possibles) all have eccentricity $\gtrsim 0.80$. Lower Panel: *Gaia* Selection Effects. The grey pixels show the distribution of samples in action space of GCs at the observed locations of GCs, but with velocities randomly drawn from isotropic Gaussians with velocity dispersion $\sigma = 130$ km s $^{-1}$. Only samples with $-1.7 < E/10^5 < -1.2$ and $|J_\phi| < 700$ km s $^{-1}$ kpc are shown. Although there is a weak bias to low J_z , it is clear that *Gaia* could have detected objects at high J_z in this energy range if they existed. The actual locations of the Sausage GCs (red) and other GCs (pale blue) with $-1.7 < E/10^5 < -1.2$ and $|J_\phi| < 700$ km s $^{-1}$ kpc are superposed.

identification of this critical energy E_{crit} as a reference level. Though the value of E_{crit} does depend on potential, the existence of a critical energy level is robust – it is the value of the most bound YH cluster. We argue that globular clusters with comparable or higher energy are all accreted from dwarf galaxies.

The bulge/disc and old halo clusters form tracks in Figs. 1 and 2. We can see that the bulge/disc clusters branch out towards positive J_ϕ , while maintaining low J_R and low J_z values, as befit disc orbits. They are entirely limited to $E \leq E_{\text{crit}}$. For the old halo clusters, we can see a similar branching towards positive J_ϕ at low energy ($E < E_{\text{crit}}$). The low energy old halo clusters are all concentrated at low J_R . In fact, there is a branch with J_R decreasing with increasing energy for the low energy old halo clusters – as is also the case for the MSTOs in Myeong et al. (2018a). In the (J_z, E) plane, the old halo

Table 1
The kinematic properties of the 8 probable and 2 possible Sausage GCs. The Galactic rest frame velocity in spherical polars, the actions in cylindrical polars, the energy and orbital eccentricity $e = (r_{\text{apo}} - r_{\text{peri}})/(r_{\text{apo}} + r_{\text{peri}})$ are all given.

| Name (NGC) | $(v_r, v_\theta, v_\varphi)$ (kms $^{-1}$) | e | (J_R, J_ϕ, J_z) (kms $^{-1}$ kpc) | E (km 2 s $^{-2}$) |
|---------------|--|------|---|-----------------------------|
| 1851 | (134.8, 11.6, 28.6) | 0.91 | (1493, -178, 230) | -134706 |
| 1904 | (46.5, -2.9, -21.5) | 0.93 | (1477, 51, 155) | -137390 |
| 2298 | (-96.1, 41.3, -57.7) | 0.79 | (949, -648, 317) | -140391 |
| 2808 | (-152.9, -35.5, -3.7) | 0.86 | (1038, 394, 35) | -152947 |
| 5286 | (-202.3, 42.4, -58.3) | 0.84 | (856, -366, 148) | -153940 |
| 6864 | (-113.0, -27.6, 24.1) | 0.83 | (1144, 316, 324) | -143397 |
| 6779 | (159.4, 19.9, -76.9) | 0.86 | (677, -182, 199) | -159799 |
| 7089 | (231.3, 24.1, 28.0) | 0.88 | (1368, -192, 309) | -139217 |
| 362 | (147.1, 7.9, -33.5) | 0.85 | (837, -57, 317) | -159510 |
| 1261 | (-113.8, 30.5, 7.2) | 0.86 | (1474, -393, 351) | -132973 |

clusters seemingly break up into two separate branches at low energy, though it is unclear whether this is caused by dynamical or selection effects.

There are 15 old halo clusters above the critical energy ($E \gtrsim E_{\text{crit}}$). Their azimuthal action J_ϕ distribution is narrower than the low energy ones. It resembles the tips of the ‘diamond-like’ contours seen in the distribution of MSTOs in the metal-rich halo (Myeong et al. 2018a). Also, the radial action J_R distribution of high energy old halo clusters is extremely distended. Most of them have high radial action, tracing out a structure similar to the picture of the metal-rich halo.

Of the 15 high energy old halo clusters, there are 6 with high vertical action ($J_z \gtrsim 1000$ km s $^{-1}$ kpc). They lie well apart from the main group. They have a wide spread in azimuthal (J_ϕ) and radial (J_R) actions, similar to the YHs suggesting an accretion origin. The main group are concentrated at large J_R , low J_z and low J_ϕ region in the action space, indicating radial orbits. They show surprisingly low vertical action ($J_z \lesssim 500$ km s $^{-1}$) – they are actually less extended in J_z than the low energy old halo clusters and much less extended than the MSTO stars with similar energy. This tight concentration, especially in J_z , is interesting since the range of J_z becomes wider as we move to higher energy, as is demonstrated by the MSTO sample. The 8 high energy OHs forming this main group (NGCs 1851, 1904, 2298, 2808, 5286, 6864, 6779 and 7089) are marked with black circles in Figs. 1 and 2. For this group of 8, the maximum J_z is ~ 360 km s $^{-1}$ kpc, the maximum $|J_\phi|$ is ~ 500 km s $^{-1}$ kpc, while the *minimum* J_R is ~ 700 km s $^{-1}$ kpc. In action space, their distribution is highly flattened and sausage-like. Interestingly, there are no old halo clusters with comparable energy that have high vertical action J_z (see e.g., the middle panel of Fig. 2). Mackey & Gilmore (2004) suggest that 15–17 per cent of the old halo clusters might have been accreted. In our picture, at least 8 Sausage GCs (or 14 including those with very high J_z) out of 53 are accreted, in rough accord with the estimate.

The young halo globular clusters all have $E > E_{\text{crit}}$, and show a broad spread in all actions. They include extreme prograde and retrograde members in the sample, as well as the ones with largest radial J_R and vertical J_z actions (excluding the Sgr GCs). The 2 black open

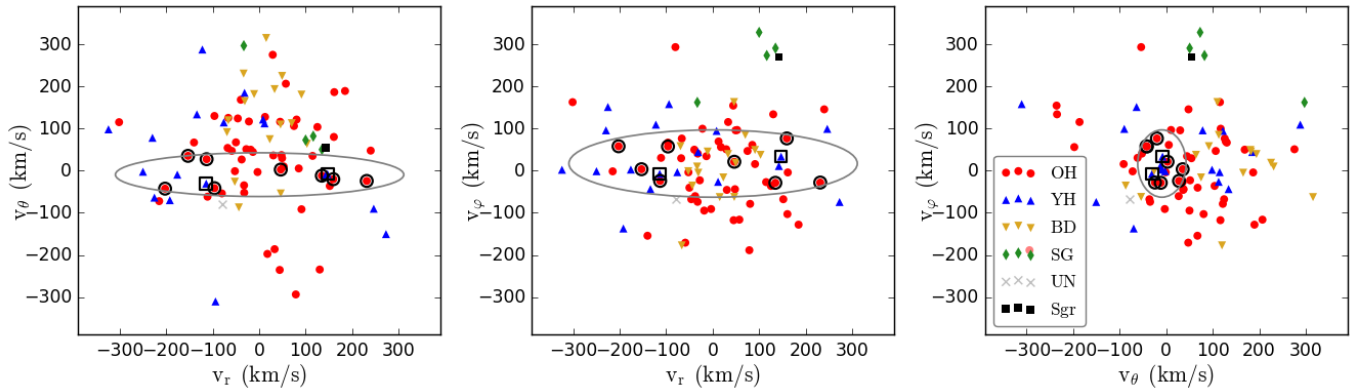


Figure 4. The velocity distribution of the GC sample, resolved with respect to spherical polar coordinates (v_r, v_θ, v_ϕ). The Sausage GCs are marked with their customary black open circles (probables) and open squares (possibles). Their extreme radial anisotropy is illustrated by the superposed ellipses with semiaxes given by the velocity dispersion in each coordinate. This plot should be compared with Fig. 2 of Belokurov et al. (2018b), which shows the sausage-like velocity distributions of main-sequence turn-off stars in the SDSS-*Gaia* catalogue.

squares in Figs. 1 and 2 provide an extended selection to the Sausage GCs. They are 2 young halo globular clusters (NGC 362, and NGC 1261) with a rather similar horizontal branch morphology to old halo clusters (see later) that also have similar actions and energy to the Sausage GCs. These are possibles rather than probables.

The upper panel of Fig. 3 shows the apocentres and pericentres of the sample, with lines of constant eccentricity superposed. The *Gaia* Collaboration et al. (2018) already noted the tendency for GCs with larger apocentres to have larger eccentricities. The 8 probable and 2 possible Sausage GCs are denoted by black open circles and open squares. They form a clump concentrated at high J_R , low J_z and low J_ϕ and they all have high orbital eccentricity $\gtrsim 0.80$. We can also see that most of the bulge/disc clusters have low eccentricity. There are also many old halo clusters with comparably low eccentricity. The young halo clusters are again widely dispersed, as they have high energy and highly spread actions.

Finally, we must consider whether selection effects could cause this. As the *Gaia* Collaboration et al. (2018) point out, GCs with high energy are more likely to be observed if they are on eccentric orbits. Even so, the middle panel of Fig. 2 demonstrates that there are no old halo clusters in this energy range that have high J_z . By taking the positions of GCs in our sample, and sampling their velocities from a Gaussian with $\sigma = 130 \text{ km s}^{-1}$, we show the expected distribution in action space in the lower panel of Fig. 3. Notice that there is only a very mild bias towards low J_z , so *Gaia* should have seen any high J_z GCs at this energy range, if they existed.

3. THE SAUSAGE GLOBULAR CLUSTERS

The properties of the 8 probable and 2 possible Sausage GCs in energy and action space are listed in Table 1.

The identification of the *Gaia* Sausage in main-sequence turn-off stars is most evident in velocity space. Belokurov et al. (2018b) show that the velocity anisotropy parameter β_{MSTO} is very extreme,

$$\beta_{\text{MSTO}} = 1 - \frac{\sigma_{v_\theta}^2 + \sigma_{v_\phi}^2}{2\sigma_{v_r}^2} \approx 0.9, \quad (1)$$

Here, v_ϕ is the azimuthal velocity in the direction of the Milky Way's rotation, v_θ is increasing towards the Milky Way's north pole and v_r is the radial velocity in spher-

ical coordinates. Given that the $\beta = 1$ implies that all orbits are linear straight lines through the Galactic Centre, then the metal-rich local halo stars are very radially anisotropic. This gives the Sausage its name, as the structure looks highly non-Gaussian and sausage-shaped in velocity space. Fig. 4 shows the velocities of the GCs resolved with respect to spherical polar coordinates. The Sausage GCs have an even more extreme value of the anisotropy parameter than the Sausage MSTOs, with $\beta_{\text{GCs}} \approx 0.95$.

The upper panel of Fig. 5 shows age versus metallicity for the Sausage GCs, as well as 7 GCs that have been claimed as associates of the the Sagittarius (Sgr), specifically Terzan 7, Terzan 8, Arp 2, Pal 12, NGC 4147, NGC 6715 and Whiting 1 (Forbes & Bridges 2010). As noted by Forbes & Bridges (2010), the age-metallicity relation for the Milky Way's GCs reveals two distinct tracks. There is broad swathe of bulge/disc and old halo globular clusters with a roughly constant old age of ~ 12.8 Gyr. This comprises the bulk of the sample. However, Forbes & Bridges (2010) pointed out that the Sgr GCs form a separate track that branches to younger ages, and is shown as open diamonds in Fig. 5. We find that the Sausage GCs similarly follow a track that is very different from the bulk of the Milky Way's *in situ* GCs. It is similar to, but vertically offset from, the Sgr track. The lower panel of Fig. 5 shows the horizontal branch index versus metallicity using data from Mackey & van den Bergh (2005). The plot emphasises the ambiguous nature of the two clusters, NGC 362, NGC 1261. Although Mackey & van den Bergh (2005) classified them as young halo clusters based on their horizontal branch morphology, they are in fact close to the dividing line. We therefore suggest that this classification can be debatable. They are kinematically close to the Sausage GCs, who may well be their true brethren.

4. DISCUSSION

This *Letter* argues that there are at least eight and possibly ten halo globular clusters that belong to a single, ancient massive merger event identified by Belokurov et al. (2018b) and responsible for the *Gaia* Sausage in velocity space.

The evidence is threefold. First, there is a strong prior expectation of finding a population of radially anisotropic GCs. Evidence for a major accretion event is pro-

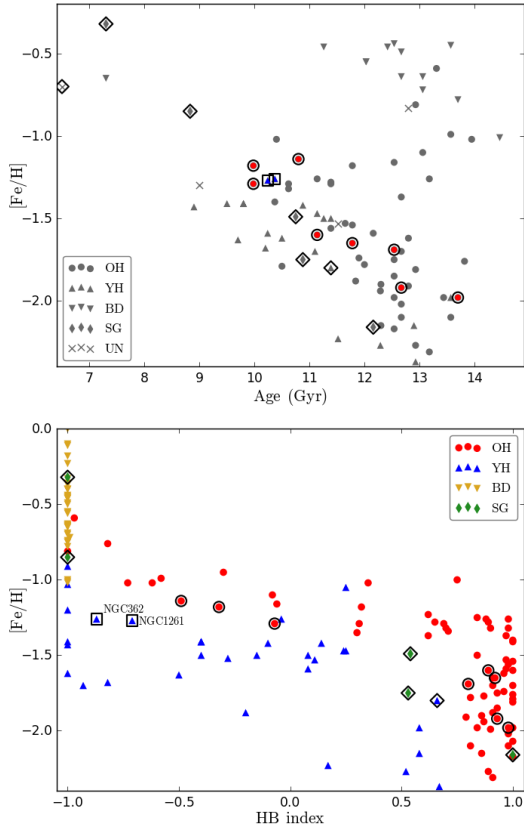


Figure 5. Upper panel: Plot of the age of GCs versus metallicity using data from Forbes & Bridges (2010). The Sausage GCs are shown with circular (probables) and square (possibles) black boundaries. 7 GCs that are claimed former denizens of the Sagittarius (Sgr) dwarf are shown as unfilled black diamonds. The sequences of Sgr GCs and Sausage GCs lie on two distinct, though closely matched, tracks. They are different from the bulk of the Milky Way GCs which show a constant age of ~ 13 Gyr independent of metallicity. Lower panel: Plot of horizontal branch morphology versus metallicity using data from Mackey & van den Bergh (2005). The locations of the two young halo clusters (NGC 362, NGC1261) are close to the boundary and their designation is open to debate. We have included them in our extended sample of Sausage GCs, as they are kinematically similar.

vid by studies of the kinematics of halo main-sequence turn-off stars in the SDSS-*Gaia* catalogue (Belokurov et al. 2018b; Myeong et al. 2018a), as well as in *Gaia* DR2 (Haywood et al. 2018). It explains the peculiar, highly non-Gaussian, radial anisotropic local velocity distribution of halo stars (hence the “*Gaia* Sausage”). The existence of the Sausage GCs supports the idea of a single event and allows us to put estimates on the mass of the progenitor. Judging from GC numbers, it must have been more massive than Fornax and comparable to the Sgr progenitor, which Gibbons et al. (2017) estimated as $5 \times 10^{10} M_{\odot}$ in total mass. This is in good agreement with the mass estimate from simulations already provided in Belokurov et al. (2018b).

Secondly, just as the GCs associated with the Sgr can be identified by their agglomeration in action space, so can the GCs associated with the “*Gaia* Sausage”. A critical energy separates the young halo clusters (which have all been accreted) from the bulge/disc clusters (which are all formed *in situ*). The old halo clusters are mainly formed *in situ*, though Mackey & Gilmore (2004) suggest that 15–17 per cent were accreted. They straddle the critical energy. Eight of the old halo clusters with

$E > E_{\text{crit}}$ form a narrow, clumped and compact distribution in action space. They have characteristic low vertical (J_z) and high radial (J_R) action. They show strong radial anisotropy ($\beta \approx 0.95$) and highly radial, eccentric orbits ($e \gtrsim 0.80$). These are exactly the characteristics expected for the Sausage GCs. There may even be 2 further members – if we, for example, permit the inclusion of young halo clusters.

Thirdly, the 8 globular clusters identified as belonging to the “*Gaia* Sausage” were chosen without any regard to their age or metallicity. However, these 8 clusters show the typical age-metallicity trend expected from dwarf spheroidals, which is additional evidence supporting their extragalactic origin. The time of infall can also be roughly reckoned from the tracks in age-metallicity space as ~ 10 Gyrs or $z \sim 3$, in accord with the estimate already provided in Belokurov et al. (2018b).

Could this peculiarity of the data be due to a selection effect, against which the *Gaia* Collaboration et al. (2018) already caution? High energy GCs are more likely to be observed if they are on eccentric orbits. In action coordinates, the eccentricity roughly scales like $(J_R + J_z)/|J_{\phi}|$. So, an eccentric orbit could have large J_R , but it could also have large J_z . However, there are no old halo clusters in this energy range that have high J_z (as the middle panel of Fig. 2 demonstrates). Nonetheless, if such GCs existed, *Gaia* should have identified them (see the lower panel of Fig. 3). This argues against the emptiness of the high J_z portion of action space being a mere selection effect.

REFERENCES

- Belokurov, V., Deason, A. J., Koposov, S. E., et al. 2018a, *MNRAS*, 477, 1472
- Belokurov, V., Erkal, D., Evans, N. W., Koposov, S. E., & Deason, A. J. 2018b, arXiv:1802.03414
- Binney, J., & Spergel, D. 1982, *ApJ*, 252, 308
- Binney, J., & Tremaine, S. 2008, *Galactic Dynamics*, 2nd edn. Princeton Univ. Press, Princeton, NJ
- Binney, J. 2012, *MNRAS*, 426, 1324
- Deason, A. J., Belokurov, V., Evans, N. W., 2011b, *MNRAS*, 416, 2903
- Deason, A. J., Belokurov, V., Evans, N. W., & Johnston, K. V. 2013, *ApJ*, 763, 113
- Forbes, D. A., & Bridges, T. 2010, *MNRAS*, 404, 1203
- Gaia* Collaboration, Helmi, A., van Leeuwen, F., et al. 2018, arXiv:1804.09381
- Gibbons, S. L. J., Belokurov, V., & Evans, N. W. 2017, *MNRAS*, 464, 794
- Goldstein, H., 1980, *Classical Mechanics*, Addison-Wesley
- Harris, W. E. 1996 (2010 edition), *AJ*, 112, 1487
- Haywood, M., Di Matteo, P., Lehnert, M., et al. 2018, arXiv:1805.02617
- Mackey, A. D., & Gilmore, G. F. 2004, *MNRAS*, 355, 504
- Mackey, A. D., & van den Bergh, S. 2005, *MNRAS*, 360, 631
- McMillan, P. J. 2017, *MNRAS*, 465, 76
- Myeong, G. C., Evans, N. W., Belokurov, V., Sanders, J. L., & Koposov, S. E. 2018a, *ApJ*, 856, L26
- Myeong, G. C., Evans, N. W., Belokurov, V., Sanders, J. L., & Koposov, S. E. 2018b, arXiv:1804.07050
- Posti, L., & Helmi, A. 2018, arXiv:1805.01408
- Sanders, J. L., & Binney, J. 2016, *MNRAS*, 457, 2107
- Schönrich, R., Binney, J., & Dehnen, W. 2010, *MNRAS*, 403, 1829
- Sohn, S. T., Watkins, L. L., Fardal, M. A., et al. 2018, arXiv:1804.01994
- Watkins, L. L., Evans, N. W., Belokurov, V., et al. 2009, *MNRAS*, 398, 1757
- Zinn, R. 1993, *The Globular Cluster-Galaxy Connection*, 48, 38